Influence of ZnO Nanoparticles on the Cure Characteristics and Mechanical Properties of Carboxylated Nitrile Rubber

Suchismita Sahoo, Anil K. Bhowmick

Rubber Technology Centre, Indian Institute of Technology, Kharagpur 721 302, India

Received 2 February 2006; accepted 6 April 2006
DOI 10.1002/app.24832
Published online 14 August 2007 in Wiley InterScience (www.interscience.wiley.com).

ABSTRACT: Zinc oxide (ZnO) nanoparticles assembled in one dimension to give rod-shaped morphology were synthesized. The effect of these ZnO nanoparticles (average particle size ~ 50 nm) as the curing agent for carboxylated nitrile rubber was studied with special attention to cure characteristics, mechanical properties, dynamic mechanical properties, and swelling. These results were compared with those of the conventional rubber grade ZnO. The study confirmed that the ZnO nanoparticles gave a better state of cure and higher maximum torque with a marginal decrease in optimum cure time and scorch time. The mechanical properties also showed an improvement. There was an increase in tensile strength by ~ 120%, elongation at break by ~ 20%, and modulus at 300% elongation by ~ 30% for the vulcanizate cured with ZnO nanoparticles, as compared with the one containing rubber grade ZnO. Dynamic mechanical analysis revealed that the vulcanizates exhibited two transitions—one occurring at lower temperature due to the T_g of the polymer, while the second at higher temperature corresponding to the hard phase arising due to the ionic structures. The second transition showed a peak broadening because of an increase in the points of interaction of ZnO nanoparticles with the matrix. The tan δ peak showed a shift towards higher T_g in the case of ZnO nanoparticle-cured vulcanizate, indicating higher crosslinking density. This was further confirmed by volume fraction of rubber in the swollen gel and infrared spectroscopic studies. J Appl Polym Sci 106: 3077–3083, 2007

Key words: zinc oxide nanoparticles; carboxylated nitrile rubber; cure characteristics; mechanical properties; dynamic mechanical properties

INTRODUCTION

The growth and development of mankind has always been closely associated with the progress of materials technology. The recent development in nanotechnology illustrates that most of the novel devices and composites of the future will be based on nanomaterials. Nanotechnology is about to spread over all the industrial fields.

Rubber industry, which plays quite an important role in the human development, is no longer left behind to incorporate nanotechnology. Nanofillers like clay and silica have already shown its beneficial effect. The preparation and properties of clay[1–5] and silica[6–8] based nanocomposites in various polymer matrices have been studied extensively by numerous researchers. The effect of some other nanoparticles like polyhedral oligomeric silsesquioxane (POSS),[9] which appear to offer potential benefits in terms of compound physical properties, has been investigated for some tire compounds.

Zinc oxide is an important inorganic pigment used in the rubber industry as a cost-effective cure activator for the sulfur vulcanization of natural and synthetic rubbers and as curing agent for some of the elastomers containing reactive functional groups such as —Cl, —COOH,[10] and so on. Conventionally used ZnO has a particle size 0.12–2.2 μm.[11] ZnO nanoparticle is an important material and effectively used in medicine, cosmetics, and other industries such as animal feedstuff, drug, ceramic, textile, commodity chemical, and paint.[12] ZnO nanoparticles are also an important material for high speed and wearable rubber product.[12] But the detailed effect of zinc oxide nanoparticles in the rubber compounds has not been reported. Hence, the aim of the present article is to prepare zinc oxide nanoparticles and a thorough investigation of their effect as curing agent for carboxylated nitrile rubber.

Correspondence to: A. K. Bhowmick (anilkb@rtc.iitkgp.ernet.in).

Journal of Applied Polymer Science, Vol. 106, 3077–3083 (2007)

EXPERIMENTAL

Synthesis and characterization of zinc oxide nanoparticles

Materials and preparation of zinc oxide nanoparticles

Laboratory grade zinc nitrate [$Zn(NO_3)_2 \cdot 6H_2O$], ammonium carbonate [$(NH_4)_2CO_3$], and ethanol were purchased from the standard sources.

$Zn(NO_3)_2 \cdot 6H_2O$ and $(NH_4)_2CO_3$ were, respectively, dissolved in distilled water to form 1.0*M* solutions. $Zn(NO_3)_2$ solution was gradually dropped into the vigorously stirred $(NH_4)_2CO_3$ solution, with a molar ratio of 1 : 2. A white precipitate was formed when the two solutions were mixed with each other, but it dissolved with stirring. Slowly a stable state of supersaturation was achieved because of the high concentration of Zn^{2+} ions in the mixed solution. The solid was collected by filtration and repeatedly rinsed with ethanol and then dried at 100°C for 12 h. ZnO nanoparticles were obtained after calcination at 280°C for 2 h. The procedure was very similar to that reported by Wang and Gao.[13]

Characterization

For characterization of ZnO nanoparticles, X-ray diffraction studies were done using Rigaku CN2005 X-ray Diffractometer ''Miniflex'' model in the range of 10–50° (=2θ). The zinc oxide powder was deposited on the sample holder uniformly.

For characterization by transmission electron microscopy (TEM, JEOL 2010), the samples were dispersed in acetone in an ultrasonic bath, a drop of it was deposited on a carbon-coated copper grid and was analyzed under an accelerating voltage of 200 kV.

The samples for AFM analysis were prepared by ultrasonically dispersing the ZnO nanoparticles powder in ethanol at 1% concentration. The dispersed sample was then deposited on the cleaned steel puck and dried at ambient conditions.

The scanning and analysis of the samples were done using the Multi-Mode Atomic Force Microscope (model MMAFMLN, Digital Instruments, Santa Barbara, CA, USA) attached with a *Nanoscope IIIa* controller. The AFM measurements were carried out in air at ambient conditions (25 ± 2°C) using 125-μm long single beam tapping mode-etched silicon probes (square pyramid in shape with a spring constant (*k*) of 20 N/m, nominal tip radius of curvature of 10 nm) with constant amplitude.

Preparation of rubber compounds and characterization

Preparation of rubber compounds

The elastomer used was carboxylated nitrile rubber (XNBR), Krynac 7.4 having an acrylonitrile content 27%, and 7.4 mol % of carboxyl groups. ZnO nanoparticles used were synthesized as per the procedure discussed in the previous section. For comparison, conventional rubber grade ZnO was used. The formulations studied are given in Table I.

All the compounds were prepared in a laboratory two-roll open mixing mill at a friction ratio of 1 : 1.2. The rolls were cooled to room temperature by continuous circulation of water.

TABLE I
Formulation and Compound Designation

Formulation	Zinc oxide used	Compound designation
XNBR: 100; ZnO: 5.0; St. acid: 1.0	Conventional rubber grade	XNBR-RG
All quantities are in parts per 100 g of rubber	Nanoparticles	XNBR-N

Cure characteristics

The curing was followed with an oscillating disc rheometer (Monsanto model 100S) at a temperature of 150°C and oscillating arc of 3°. The rubber compounds were cured in a hydraulic press at 150°C at the optimum cure time calculated from the rheographs. The cure rate index (CRI), which is the measure of the cure reaction, was calculated from the following expression:

$$\mathrm{CRI} = 100/(t_{90} - t_2) \quad (1)$$

where t_{90} is the optimum cure time and t_2 is the scorch time calculated from the rheographs.

Morphology and dispersion

The dispersion of zinc oxide in the rubber matrix was studied by using JEOL JSM-5800 scanning electron microscope (SEM) operating at an accelerating voltage of 20 kV. The molded samples were sputter coated with gold. For EDAX analysis, the photographs were taken at 200× magnifications.

AFM analysis of one optimized composition was done to check particle size and dimension in the nanocomposites. A fresh surface was sliced from the bulk of the molded vulcanized sample for AFM analysis. The measurement conditions were same as described in Characterization section.

Mechanical and dynamic mechanical properties

The tensile properties of the compounds were measured on a Universal Testing Machine (Hounsfield 10KS) at a cross-head speed of 500 mm/min at room temperature according to ASTM D 412-98. Tensile strength, tensile modulus, and elongation at break were recorded. The average values of three tests are reported for each sample.

The dynamic mechanical thermal analysis of the rubber composites with zinc oxide nanoparticles and conventional rubber grade zinc oxide were carried out by using a DMTA IV (Rheometric Scientific, NJ, USA) dynamic mechanical thermal analyzer. The sample

specimens (30 mm × 10 mm × 1.5 mm) were tested in tensile mode at a constant frequency of 1 Hz, at 0.01% strain and in the temperature range of −40 to 80°C at a heating rate of 2°C/min. The data were analyzed using RSI Orchestrator application software on an ACER computer attached to the machine. Storage modulus (E'), loss modulus (E''), and loss tangent (tan δ) were measured as a function of temperature under identical conditions for all the representative samples. The temperature corresponding to tan δ peak was taken as the glass transition temperature (T_g).

Swelling studies

The volume fraction (V_r) of the rubber swollen in methyl ethyl ketone (MEK) to equilibrium was calculated from the following expression:

$$V_r = \frac{[(D - FT_1)\rho_r^{-1}]}{[(D - FT_1)\rho_r^{-1}] + A_0\rho_s^{-1}} \quad (2)$$

where V_r is the volume fraction of rubber; D, the deswollen weight; F, the fraction insoluble; T_1, initial weight; A_0, the amount of solvent imbibed; ρ_r, density of rubber; and ρ_s is the density of solvent.

IR spectroscopy

To find out the extent of interaction between ZnO and the reactive group in the rubber (—COOH), FTIR spectroscopy (FTIR NICOLET NEXUS^{TM} model in attenuated total reflectance mode using 45° KRS 5 prism at room temperature) was used in the range of 4000–650 cm^{-1}.

RESULTS AND DISCUSSION

Characterization of ZnO nanoparticles

Figure 1 illustrates the TEM and AFM micrographs of ZnO nanoparticles. Figure 1(a, b) shows that some of

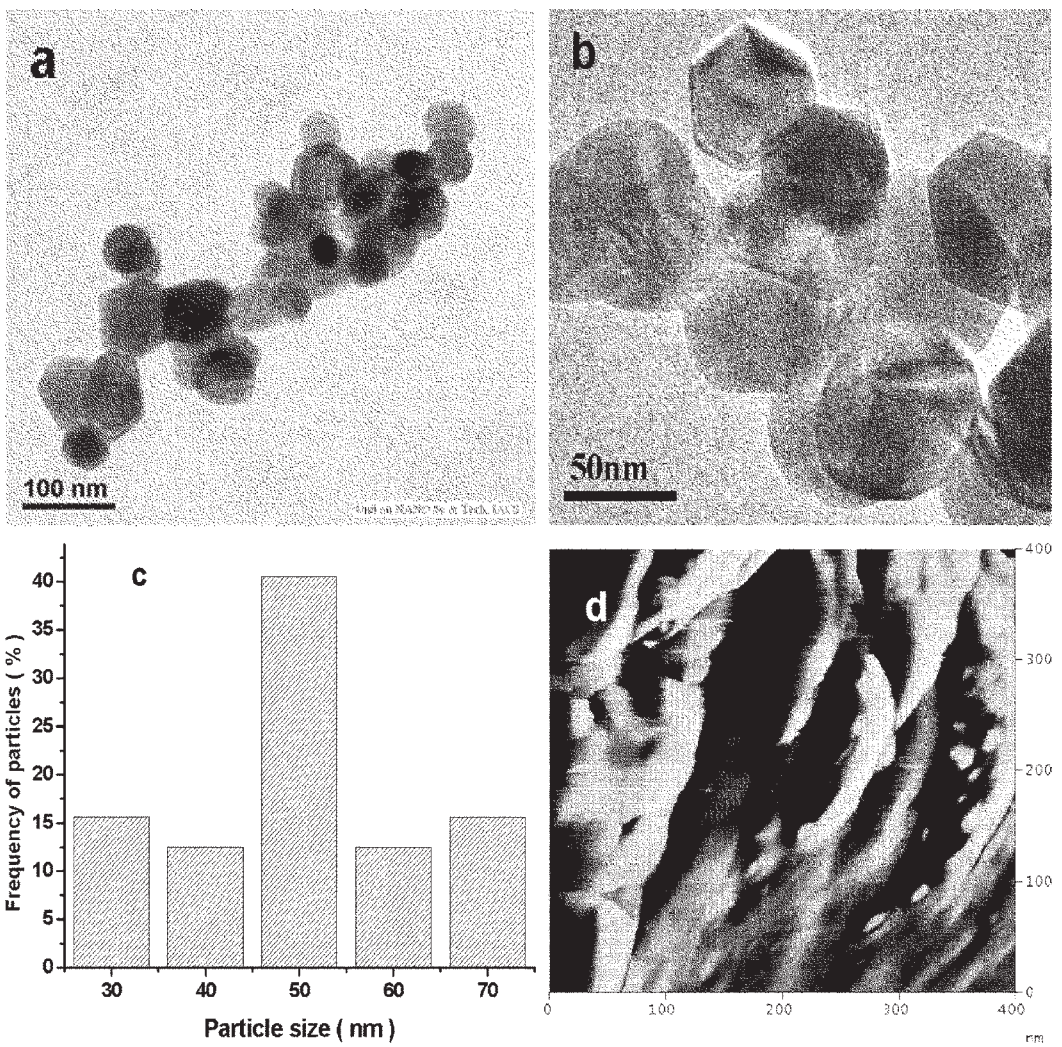

Figure 1 ZnO nanoparticles assemblies: (a) TEM micrograph, (b) enlarged view of the nanoparticles, (c) particle size distribution from TEM micrographs, and (d) AFM micrograph of ZnO powder.

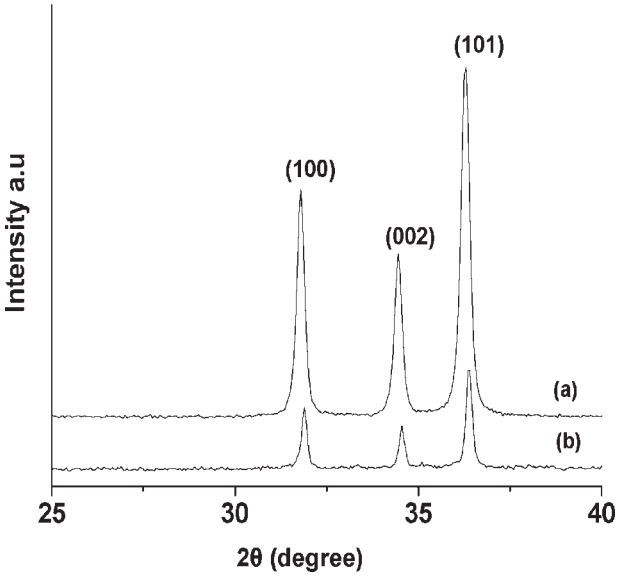

Figure 2 XRD patterns of ZnO nanoparticles synthesized at (a) $C_Z = C_N = 1.0M$, $R = 1:2$; (b) XRD pattern of conventional rubber grade ZnO, where C_Z and C_N denote the concentration of zinc nitrate and ammonium carbonate respectively, and R denotes the molar ratio of zinc nitrate to ammonium carbonate solution.

the ZnO nanoparticles are polyhedral and some are spherical with an average dimension of 50 nm. The size of the particles has been analyzed by using the ''image tool 3.0'' software and the results are presented in Figure 1(c). It is also observed that the ZnO nanoparticles almost aggregate in one dimension forming rod-like shapes and the length of the rods varies from 400 to 600 nm with a width ranging from 50 to 100 nm. The observations are further confirmed by AFM [Fig. 1(d)], which reveals that the rod-like aggregations of ZnO nanoparticles have an average diameter of 25–50 nm and a length of 300–500 nm. ZnO conventionally used in the rubber industry has a particle dimension varying from 0.12 to 2.2 μm.[11]

The X-ray diffractograms of the zinc oxide nanoparticles and rubber grade ZnO are illustrated in Figure 2(a, b) respectively. All the peaks obtained can be well indexed to the zincite phase of zinc oxide. Both the rubber grade ZnO and the synthesized ZnO nanoparticles give peaks at approximately similar positions, which are in accord with the literature values (JCPDS Card No. 36-1451). There is no noticeable change in the crystallographic patterns. The peak heights for the synthesized ZnO nanoparticles are higher due to the orderly arrangement of the ZnO nanocrystals in one dimension to rod-shaped morphology. The observation is further supported by the TEM and AFM micrographs [Fig. 1(a, b)]. The average crystallite size has been calculated by using Scherrer equation:[14]

$$D = \frac{K\lambda}{\beta \cos\theta} \tag{3}$$

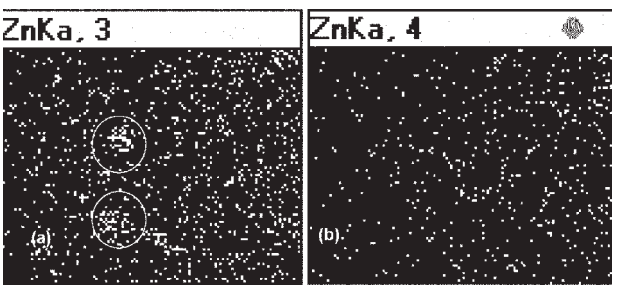

Figure 3 X-ray dot mapping of Zn in the XNBR vulcanizates containing (a) conventional rubber grade ZnO and (b) ZnO nanoparticles (200×).

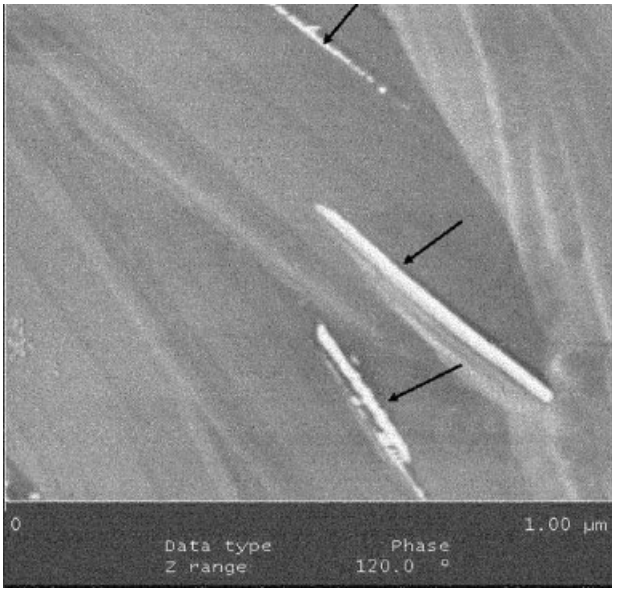

Figure 4 AFM image of ZnO nanoparticles in the XNBR matrix.

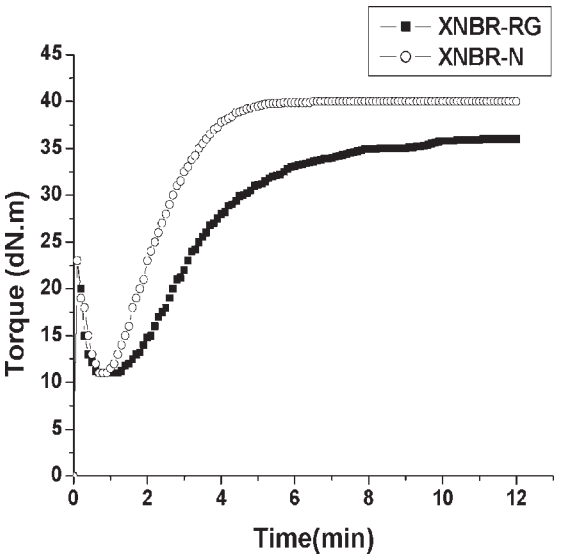

Figure 5 Cure curves for XNBR compounds.

TABLE II
Cure Characteristics of XNBR Cured with ZnO Nanoparticles and Conventional Rubber Grade ZnO

	XNBR-RG	XNBR-N
M_h (dN m)	36.0	40.0
$M_h - M_0$ (dN m)	25.0	29.0
Optimum cure time (min)	6.7	4.6
Scorch time (min)	1.7	1.2
Cure rate index (% min^{-1})	20.0	29.4

where β is the integral half-width, K is a constant approximately equal to unity, λ is the wavelength of the incident X-ray (λ = 0.15406 nm), D is the crystallite size, and θ is the Bragg angle of diffraction lines.

The average crystallite size has been calculated to be 3.78 nm for the synthesized ZnO nanoparticles, whereas it is 5.00 nm for the rubber grade ZnO. It should be noted that crystallite size is assumed to be the size of a coherently diffracting domain. It is not necessarily the same as the particle size.[15]

Morphology and properties of rubber nanocomposites

Morphology and dispersion

From the SEM and X-ray mapping of Zn in the XNBR vulcanizates shown in Figure 3, it is observed that dispersion is better in the case of ZnO nanoparticles, as compared to the conventional rubber grade ZnO. Agglomeration of latter (indicated by circles) is observed at some points, whereas ZnO nanoparticles particles are uniformly distributed.

Figure 4 shows the AFM image of the ZnO nanoparticles in the matrix of XNBR. It is clearly observed that the aggregations of ZnO nanoparticles into rod-shape morphology retain its identity in the rubber matrix with length varying from 400 to 600 nm and width 25 to 50 nm.

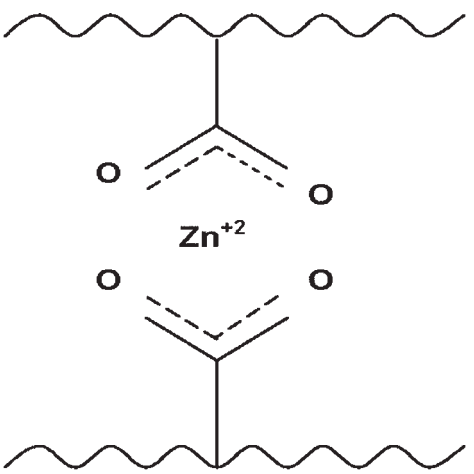

Scheme 1 Interaction of Zn^{2+} with —COOH of XNBR.

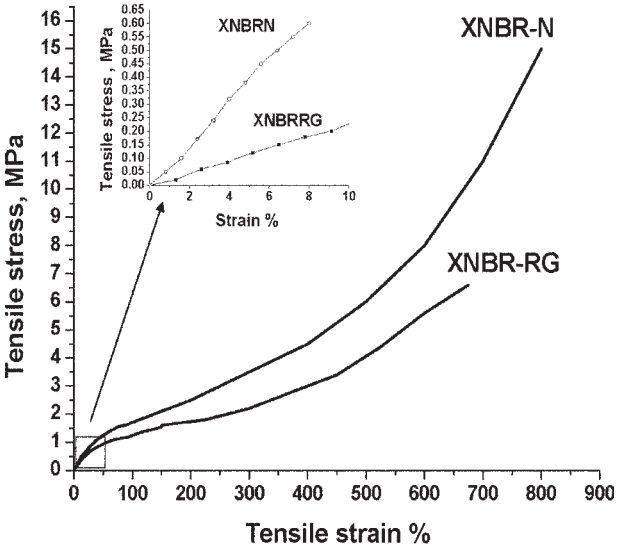

Figure 6 Tensile stress–strain plot of XNBR vulcanizates.

Cure characteristics

The cure curves of two compounds—one with conventional rubber grade ZnO and another with ZnO nanoparticles are shown in Figure 5, and various parameters calculated from these curves are given in Table II. The maximum torque value (M_h) is observed to increase by ~ 11% for the system with ZnO nanoparticles in comparison with that with the conventional rubber grade ZnO, indicating a better state of cure of the former. The difference in maximum and minimum torques ($M_h - M_0$), which is a measure of the modulus of the compound, also increases with the addition of ZnO nanoparticles.

ZnO forms crosslinking with the carboxylated nitrile rubber. To effectively crosslink XNBR, ZnO must dissolve in the rubber and diffuse to the carboxyl groups to react effectively (Scheme 1). This process is faster when the ZnO particle dimension is smaller as observed from the increase in the rate of cure reaction. The CRI increases by ~ 45% with the

TABLE III
Tensile Properties and V_r of XNBR Vulcanizates

	XNBR-RG	XNBR-N
Tensile strength (MPa)	6.8	14.9
Elongation at break (%)	680	800
Modulus at 100% elongation (MPa)	1.3	1.7
Modulus at 200% elongation (MPa)	1.7	2.4
Modulus at 300% elongation (MPa)	2.2	3.2
Young's modulus (MPa)	0.02	0.08
Volume fraction of rubber in the swollen gel (V_r)	0.180 ± 0.005	0.210 ± 0.006

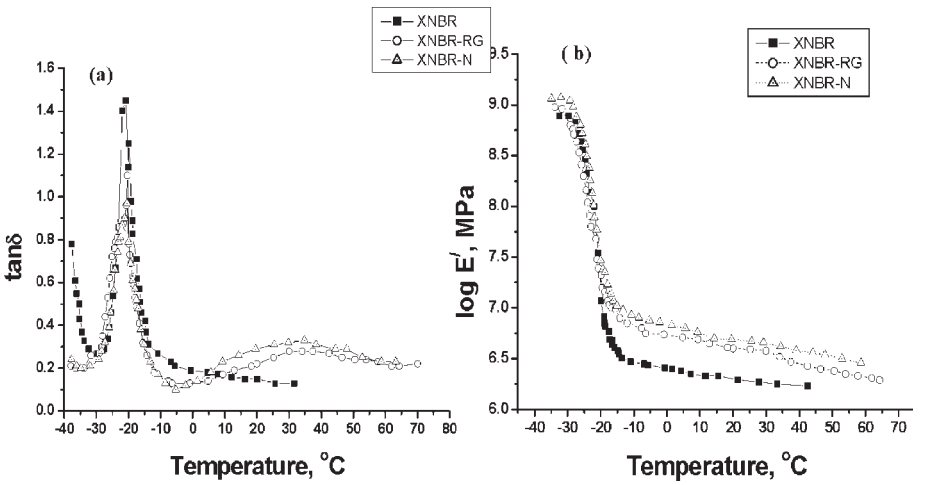

Figure 7 (a) Plot of tan δ versus temperature and (b) plot of log E' versus temperature.

ZnO nanoparticles, which supports the activation of the reaction due to better dispersion and dissolution of ZnO nanoparticles in the rubber matrix as compared to the conventional rubber grade ZnO. Both the optimum cure time and the scorch time decrease by ~ 30% with the decrease in particle dimension from microscale to nanoscale. Hence, ZnO level can be decreased in the conventional formulations to achieve characteristics similar to that of the conventional rubber grade ZnO with the use of ZnO nanoparticles.

Mechanical properties

The characteristic stress–strain plots are shown in Figure 6 and the mechanical properties are given in Table III. It is observed that the stress value at a particular strain shows an increase with ZnO nanoparticles in the vulcanizate. Surprisingly, the strain at break increases simultaneously with modulus with the reduction in ZnO particle dimension. It has been reported that elongation is an inverse function of modulus.[16] The characteristics, which improve modulus, also act to reduce elongation properties. Elongation is penalized through the use of finer particle size in the case of synthetic rubbers.[16] The decrease in particle dimension also results in vulcanizates with improved tensile strength as shown in Table III. There is an increment in tensile strength by ~ 120%, elongation at break by ~ 20%, and modulus at 300% elongation by ~ 30%. Also, the Young's modulus of the vulcanizate cured with ZnO nanoparticles is four times higher than that of the vulcanizate cured with rubber grade ZnO. This is because of the larger number of interactions between the ZnO nanoparticles and the —COOH groups, as shown in Scheme 1. The increase in the value of modulus at 300% elongation as well as Young's modulus may be attributed to the increase in crosslinking density, which is discussed later.

Dynamical mechanical testing analysis

Figure 7(a, b) illustrates the plot of tan δ and log E' as a function of temperature respectively, for the neat XNBR sample and XNBR vulcanizates cured by rubber grade ZnO and ZnO nanoparticles. The values of tan δ and log E' at three different temperatures i.e., 25°C, –25°C, and at T_g are recorded in Table IV. The neat XNBR sample gives only one transition corresponding to the glass transition temperature of the polymer, whereas the ZnO-cured vulcanizates exhibit an additional transition at higher temperature [Fig. 7(a)]. This may be attributed to the hard phase arising because of the formation of ionic clusters or conglomerates.[17] Multiple cluster model forms the basis of the morphological structure of the ionomers,[17] according to which the mobility of the polymer chains is restricted around the aggregates of the ionic salts giving rise to a hard phase. Clusters can be formed from the association of the multiplets.[18] The electrostatic interaction between the multiplets favors the association. Therefore, the immobility in polymer chains results in a marginal increase in glass transition temperature from −22.0 to −20.0°C for the vulcanizate cured with ZnO nanoparticles and −20.5°C for the vulcanizates having rubber grade ZnO. There is a marginal shift in the tanδ peak. However, there is decrease of the tan δ peak height from 1.45 for neat

TABLE IV
Storage Modulus and tan δ at Three Different Temperatures and the T_g Value of the Neat XNBR and ZnO-cured XNBR Vulcanizates

Compound designation	log E' (MPa)			tan δ			T_g
	−25°C	T_g	25°C	−25°C	T_g	25°C	(°C)
XNBR	8.13	7.36	6.26	0.53	1.45	0.13	−22.0
XNBR-RG	8.30	7.68	6.52	0.52	1.10	0.25	−20.5
XNBR-N	8.72	8.01	6.67	0.46	0.90	0.31	−20.0

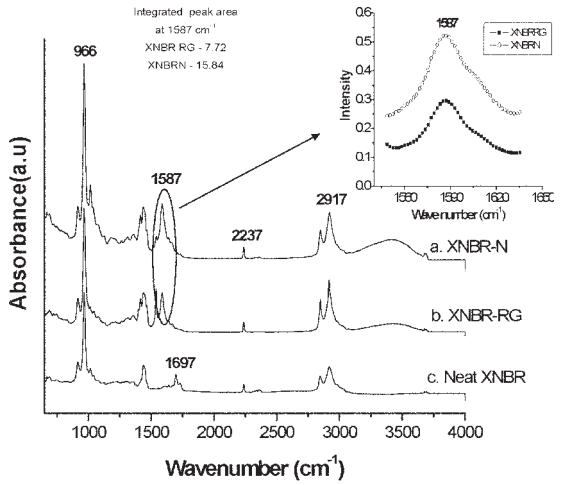

Figure 8 IR spectra of (a) XNBR-N, (b) XNBR-RG, and (c) Neat XNBR.

XNBR to 1.10 for the XNBR vulcanizate cured by conventional rubber grade ZnO and 0.90 for the vulcanizate cured with ZnO nanoparticles at the glass transition temperature. These values are reported in Table IV. A similar observation is made in our earlier communication on clay–rubber nanocomposites.[19] It is also interesting to note that the storage modulus at room temperature displays a considerable increase by $\sim$ 25%, when the two vulcanizates are compared.

Fourier transform infrared spectroscopy

The FTIR spectra are shown in Figure 8. The peaks at 966 cm^{-1} due to the butadiene part, at 2237 cm^{-1} due to —CN group, and at 2917 cm^{-1} due to the —C—H stretching vibration are observed for all the XNBR samples. The peak for —COOH appearing at 1697 cm^{-1} in the case of neat XNBR is shifted to 1587 cm^{-1} for the sample cured with ZnO. The peak at 1587 cm^{-1} reflects formation of ionic clusters between —COOH groups and Zn^{2+} ion of ZnO. When the compound is cured with ZnO nanoparticles, the peak area increases by 50%, which indicates an increase in interaction.

Swelling studies

The V_r values of the corresponding vulcanizates are reported in Table III. The results show that there is a greater volume fraction of rubber (V_r) (proportional to crosslinking density) for the compound vulcanized with ZnO nanoparticles ($V_r = 0.210$) than those vulcanized by conventional rubber grade ZnO ($V_r = 0.180$). Hence, the increased V_r value of ZnO nanoparticles cured vulcanizate (an increment of $\sim$ 20%) over the vulcanizate cured with rubber grade ZnO supports the earlier observation of greater interaction and improved mechanical properties with the former.

CONCLUSIONS

Influence of zinc oxide nanoparticles as curing agent of XNBR on cure characteristics, mechanical, and dynamic mechanical properties and swelling behavior has been investigated. The substitution of conventional rubber grade zinc oxide by zinc oxide nanoparticles is accompanied with an increase in cure rate and maximum torque value of XNBR. This is due to greater interaction of zinc oxide nanoparticles. Mechanical properties are also improved, which can be explained on the basis of better dispersion, observed by SEM-EDAX and chemical interaction between —COOH and ZnO nanoparticles, as evident from the FTIR spectra. Dynamic mechanical studies indicate improved modulus at 25°C and reduced tan δ maximum. A marginal shift in the glass transition temperature is observed from the tan δ curve of zinc oxide nanoparticles cured XNBR vulcanizate. Hence, it can be concluded from the present study that zinc oxide nanoparticles effectively crosslinks XNBR with great improvement in properties.

The authors are thankful to Mr. Anirban Ganguly, Ms. Madhuchhanda Maiti and Mr. Jinu Jacob George from the Rubber Technology Centre for their help rendered during Atomic Force Microscopy, FTIR, and DMTA studies.

References

1. Lan, T.; Pinnavaia, T. J Chem Mater 1999, 6, 2216.
2. Kojima, Y.; Usuki, A.; Kawasumi, M.; Okada, A.; Kurauchi, T.; Kamigaito, O. J Appl Polym Sci 1993, 49, 1259.
3. Sadhu, S.; Bhowmick, A. K. Rubber Chem Technol 2003, 76, 860.
4. Kojima, Y.; Usuki, A.; Kawasumi, M.; Okada, A.; Kurauchi, T.; Kamigaito, O.; Kaji, K. J Polym Sci Part B: Polym Phys 1995, 33, 1039.
5. Sinha Ray, S.; Okamoto, M. Prog Polym Sci 2003, 28, 1539.
6. Okada, A.; Usuki, A.; Mater Sci Eng C 1995, 3, 109.
7. Bandyopadhyay, A.; Bhowmick, A. K.; Sarkar, M. D. J Appl Polym Sci 2004, 93, 2579.
8. Bandyopadhyay, A.; De Sarkar, M.; Bhowmick, A. K. Rubber Chem Technol 2004, 77, 830.
9. http://www.kumho-euro.com/eurotech/binary/nanoparticles.pdf. Accessed on 30th October 2005.
10. Morton, M. In Rubber Technology; Stephens, H. L., Ed.; Van Nostrand Reinhold: New York, 1987; p 43.
11. http://www.reade.com/Products/Oxides/zinc_oxide.html. Accessed on 22nd December 2005.
12. http://nano-infinity.tradenet.com.tw/application.htm. Accessed on 30th October 2005.
13. Wang, J.; Gao, L. Inorg Chem Commun 2003, 6, 877.
14. Klug, H. P.; Alexandar, L. E. X-ray Diffraction Procedures for Polycrystalline and Amorphous Materials; Wiley: New York, 1962.
15. http://www.shef.ac.uk/materials/about/facilities/x-raydiffraction/analysis.html. Accessed on 10th January 2006.
16. Morton, M. Introduction to Rubber Technology; Reinhold Publishing: New York, 1959; p 205.
17. Eisenberg, A.; Hird. B.; Moore, R. B. Macromolecules 1990, 23, 4098.
18. Bhowmick, A. K.; Stephens, H. L., Eds. In Handbook of Elastomers, Marcel Dekker: New York; 2001.
19. Sadhu, S.; Bhowmick, A. K. Rubber Chem Technol 2005, 78, 321.